UCHEP-04-01

Constraints upon the CKM angle ϕ_2 from Belle and BaBar

A. J. Schwartz[a]

[a] Physics Department
University of Cincinnati
P.O. Box 210011
Cincinnati, Ohio 45221

The Belle and BaBar experiments have measured branching fractions and CP asymmetries in the charmless decay modes $B^0 \to \pi^+\pi^-$, $B^0 \to \rho^\pm\pi^\mp$, and $B^0 \to \rho^+\rho^-$. From these measurements, contraints upon the CKM angle ϕ_2 can be obtained. These constraints consistently indicate that ϕ_2 is around 100°.

1. INTRODUCTION

The Standard Model predicts CP violation to occur in B^0 meson decays owing to a complex phase in the 3×3 Cabibbo-Kobayashi-Maskawa (CKM) mixing matrix. This phase is illustrated by plotting the unitarity condition $V_{ub}^*V_{ud} + V_{cb}^*V_{cd} + V_{tb}^*V_{td} = 0$ as vectors in the complex plane: the phase results in a triangle of nonzero height. One interior angle of the triangle, denoted ϕ_1 or β, is determined from $B^0 \to J/\psi\, K^0$ decays.[1] Another interior angle, ϕ_2 or α, is determined from charmless decays such as $B^0 \to \pi^+\pi^-$, $B^0 \to \rho^+\pi^-$, and $B^0 \to \rho^+\rho^-$. To determine ϕ_2 requires measuring time-dependent decay rates; here we present such measurements from the Belle [1] and BaBar [2] experiments.

In neutral B meson decays, CP violation arises predominantly because of interference between a $B^0 \to f$ decay amplitude and a $B^0 \to \overline{B}{}^0 \to f$ amplitude. For the final states considered here, there are two decay amplitudes possible: a $b \to u$ "tree" and a $b \to d$ "penguin" (see Fig. 1). Because these amplitudes have different weak phases, additional information is needed to determine ϕ_2, such as the size of the penguin amplitude or the difference in strong phases between the penguin and tree amplitudes.

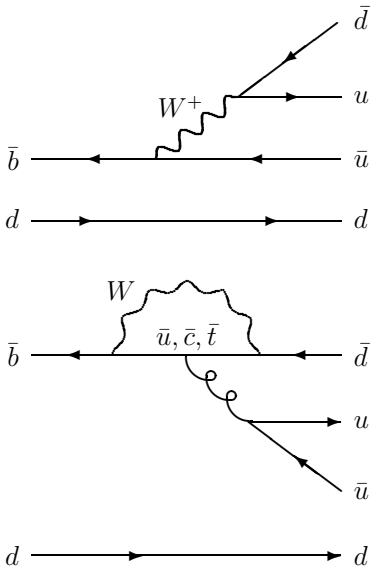

Figure 1. Tree-level diagram (top) and penguin diagram (bottom) for $B^0 \to \pi^+\pi^-$, $B^0 \to \rho^+\pi^-$, and $B^0 \to \rho^+\rho^-$ decays.

[1] Charge-conjugate modes are included throughout this paper unless noted otherwise.

2. ANALYSIS

The analyses of $B^0 \to \pi^+\pi^-$, $B^0 \to \rho^+\pi^-$, and $B^0 \to \rho^+\rho^-$ decays have several similarities. Events are selected by requiring two opposite-charge pion-candidate tracks originating from the interaction region, and appending zero, one, or two π^0's. The charged pion identification criteria are based on information from either a DIRC detector (BaBar) [3] or time-of-flight counters and aerogel cherenkov counters (Belle) [4]. Both experiments also use dE/dx information from the central tracking chamber.

B decays are identified via two kinematic variables: the "beam-constrained" mass, $m_{\rm bc}$, and the energy difference, ΔE. The former is defined as $\sqrt{E_b^2 - p_B^2}$ and the latter as $E_B - E_b$, where p_B is the reconstructed B momentum, E_B is the reconstructed B energy, and E_b is the beam energy, all evaluated in the e^+e^- center-of-mass (CM) frame. After selection cuts, the $m_{\rm bc}$ and ΔE distributions are jointly fit for the signal event yields. This fit includes contributions from backgrounds, whose $m_{\rm bc}$-ΔE distributions are obtained from either Monte Carlo (MC) simulation or extrapolation from $m_{\rm bc}$-ΔE sidebands.

A tagging algorithm is used to identify the flavor of the B signal decay, i.e., whether it is B^0 or $\overline{B}{}^0$. This algorithm examines tracks not associated with the signal decay to identify the flavor of the non-signal B. It depends predominantly on identifying leptons or kaons. The signal-side tracks are fit for a signal decay vertex, and the tag-side tracks are fit for a tag-side decay vertex; the distance Δz between vertices is to good approximation proportional to the time difference between the B decays: $\Delta z \approx (\beta\gamma c)\Delta t$, where $\beta\gamma$ is the Lorentz boost of the e^+e^- system and equals 0.43 (0.56) for Belle (BaBar). One subsequently does an unbinned maximum likelihood (ML) fit to Δt to measure or constrain ϕ_2.

The dominant background for all three decays is $e^+e^- \to q\bar{q}$ continuum events, where $q = u, d, s, c$. To distinguish such events from $e^+e^- \to B\overline{B}$ events, the event topology is used: in the CM frame, continuum events tend to be collimated along the beam directions while $B\overline{B}$ events tend to be spherical. In Belle, the "shape" of an event is typically quantified via Fox-Wolfram moments [5] of the form $h_\ell = \sum_{i,j} p_i\, p_j\, P_\ell(\cos\theta_{ij})$, where i runs over all tracks on the tagging side and j runs over all tracks on either the tagging side or the signal side. The function P_ℓ is the ℓth Legendre polynomial and θ_{ij} is the angle between momenta $\vec{p_i}$ and $\vec{p_j}$. These moments are combined into a Fisher discriminant [6], and the discriminant is subsequently combined with the probability density function (pdf) for the cosine of the angle between the B direction and the electron beam direction. This yields an overall likelihood $\mathcal{L}$, which is evaluated for both a $B\overline{B}$ hypothesis and a continuum hypothesis. Signal $B \to f$ events are separated from continuum events by cutting on the likelihood ratio $\mathcal{L}_{B\overline{B}}/(\mathcal{L}_{B\overline{B}} + \mathcal{L}_{q\bar{q}})$.

In BaBar, $B \to f$ signal is separated from continuum background using several methods. For $B^0 \to \pi^+\pi^-$, a cut $|\cos\theta_{\rm sph}| < 0.8$ is imposed, where $\theta_{\rm sph}$ is the angle between the sphericity axis of the B candidate and that of the rest of the event. A Fisher discriminant ($\mathcal{F}$) is then constructed from $\sum_i p_i$ and $\sum_i p_i|\cos\theta_i|^2$, where p_i is the momentum of particle i, θ_i is the angle between $\vec{p_i}$ and the B thrust axis (both evaluated in the e^+e^- CM frame), and i runs over all particles not associated with the B decay. A pdf for $\mathcal{F}$ is included in the ML fit to Δt. For $B^0 \to \rho^+\pi^-$ and one [7] of two $B^0 \to \rho^+\rho^-$ analyses, a neural network is used that includes the two event-shape variables from $\mathcal{F}$. The output of the neural network is included in the Δt fit. For the other $B^0 \to \rho^+\rho^-$ analysis [8], a cut $|\cos\theta_{\rm th}| < 0.8$ is made, where $\theta_{\rm th}$ is the angle between the thrust axis of the B candidate and that of the rest of the event. The analysis subsequently uses a Fisher discriminant constructed from 11 observables.

3. $B^0 \to \pi^+\pi^-$

The decay time dependence of $B^0/\overline{B}{}^0 \to \pi^+\pi^-$ decays is given by [9]

$$\frac{dN}{d\Delta t} \propto e^{-\Delta t/\tau}\Big[1 - q\,\mathcal{C}_{\pi\pi}\cos(\Delta m\Delta t) + q\,\mathcal{S}_{\pi\pi}\sin(\Delta m\Delta t)\Big], \quad (1)$$

where $q = +1$ ($q = -1$) corresponds to B^0 ($\overline{B}{}^0$) tags, and Δm is the B^0-$\overline{B}{}^0$ mass difference. The parameters $\mathcal{C}_{\pi\pi}$ and $\mathcal{S}_{\pi\pi}$ are CP-violating and related to ϕ_2 via [10]

$$\mathcal{C}_{\pi\pi} = \frac{1}{R}\cdot\left(2\left|\frac{P}{T}\right|\sin(\phi_1-\phi_2)\sin\delta\right) \quad (2)$$

$$\mathcal{S}_{\pi\pi} = \frac{1}{R}\cdot\left(2\left|\frac{P}{T}\right|\sin(\phi_1-\phi_2)\cos\delta + \sin 2\phi_2 - \left|\frac{P}{T}\right|^2\sin 2\phi_1\right) \quad (3)$$

$$R = 1 - 2\left|\frac{P}{T}\right|\cos(\phi_1+\phi_2)\cos\delta + \left|\frac{P}{T}\right|^2 , \quad (4)$$

where $\phi_1 = (23.2^{+1.6}_{-1.5})^\circ$ [11], $|P/T|$ is the magnitude of the penguin amplitude relative to that of the tree amplitude, and δ is the strong phase difference between the two amplitudes. If there were no penguin contribution, $P = 0$, $\mathcal{C}_{\pi\pi} = 0$, and $\mathcal{S}_{\pi\pi} = \sin 2\phi_2$. Since Eqs. (2) and (3) have three unknown parameters, measuring $\mathcal{C}_{\pi\pi}$ and $\mathcal{S}_{\pi\pi}$ determines a volume in ϕ_2 - δ - $|P/T|$ space.

The most recent Belle measurement of $\mathcal{C}_{\pi\pi}$ and $\mathcal{S}_{\pi\pi}$ is with 140 fb^{-1} of data [12]. Candidates must satisfy $5.271\ \mathrm{GeV}/c^2 < m_{\mathrm{bc}} < 5.287\ \mathrm{GeV}/c^2$ and $\Delta E < 0.064$ GeV; the final event sample consists of 224 $\overline{B}{}^0 \to \pi^+\pi^-$ candidates and 149 $B^0 \to \pi^+\pi^-$ candidates after background subtraction. The ratio of signal to background is ~ 0.3. These events are subjected to an unbinned ML fit to Δt, in which additional pdf's and resolution functions are included to account for backgrounds. There are two free parameters in the fit, and the results are $\mathcal{C}_{\pi\pi} = -0.58 \pm 0.15\,(\mathrm{stat}) \pm 0.07\,(\mathrm{syst})$ and $\mathcal{S}_{\pi\pi} = -1.00 \pm 0.21\,(\mathrm{stat}) \pm 0.07\,(\mathrm{syst})$. These values are consistent with previous Belle measurements [13] and indicate large CP violation. Fig. 2 shows the Δt distributions for the $q = \pm 1$ samples; a clear difference is seen between the distributions. Many cross-checks have been done for this analysis, including an independent "blind" analysis using a binned ML fit. The latter results are very close to those of the main fit.

The Belle values for $\mathcal{C}_{\pi\pi}$ and $\mathcal{S}_{\pi\pi}$ prescribe a 95% C.L. volume in ϕ_2 - δ - $|P/T|$ space. Slicing this volume at fixed $|P/T|$ gives a 95% C.L. constraint in the ϕ_2-δ plane; slicing this volume at

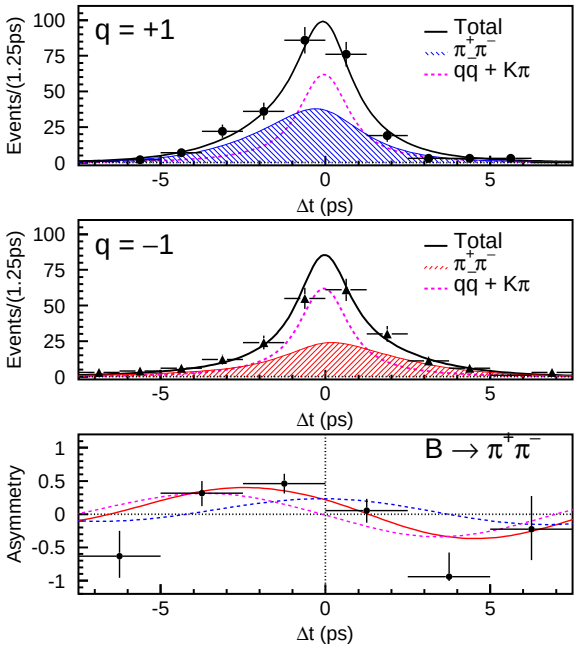

Figure 2. Belle results for $B^0 \to \pi^+\pi^-$ [12]: the Δt distributions of $q = 1$ tags (top), $q = -1$ tags (middle), and the resulting CP asymmetry (bottom). The smooth curves are projections of the unbinned ML fit.

fixed δ gives a constraint in the ϕ_2-$|P/T|$ plane. Two such projections are shown in Figs. 3a and 3b; the resulting constraints are $90^\circ < \phi_2 < 146^\circ$ for $|P/T| < 0.45$ (as predicted by QCD factorization [14] and perturbative QCD [15]), and $|P/T| > 0.17$ for any value of δ.

The BaBar experiment has also measured $\mathcal{C}_{\pi\pi}$ and $\mathcal{S}_{\pi\pi}$ using an unbinned ML fit [16]. The most recent result is from 205 fb^{-1} of data [17]; the values obtained are $\mathcal{C}_{\pi\pi} = -0.09 \pm 0.15\,(\mathrm{stat}) \pm 0.04\,(\mathrm{syst})$ and $\mathcal{S}_{\pi\pi} = -0.30 \pm 0.17\,(\mathrm{stat}) \pm 0.03\,(\mathrm{syst})$. These values are inconsistent with the Belle result at the level of 3.2σ [11]. The BaBar analysis differs from that of Belle in that fewer cuts are made to enrich the data sample; rather, additional pdf's for the discriminating variables are included in the likelihood function. A total of 68 030 events are fit, and a signal yield of 467 ± 33 $B^0 \to \pi^+\pi^-$ decays is obtained. There are 46 free

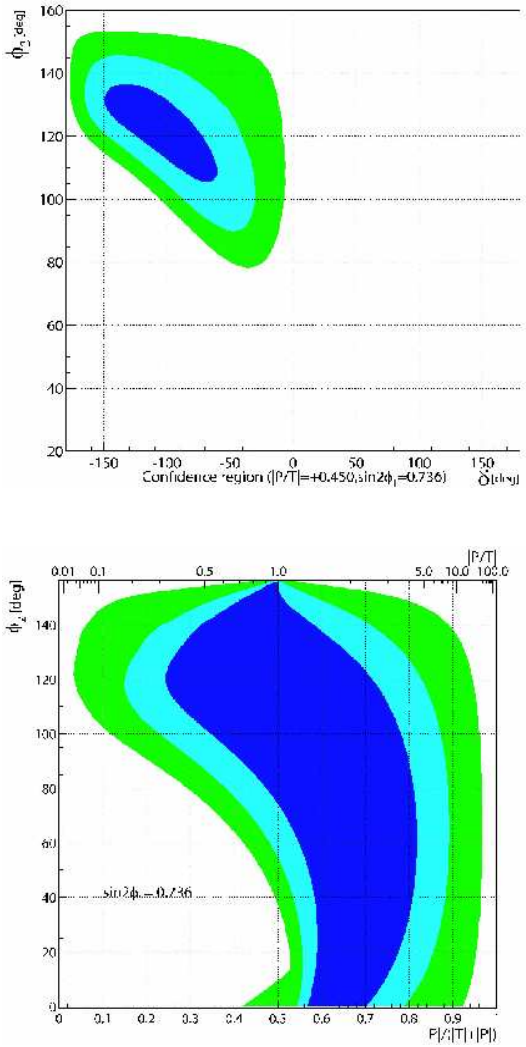

Figure 3. Belle results for $B^0 \to \pi^+\pi^-$: *(a)* constraints in the ϕ_2-δ plane for $|P/T| < 0.45$; and *(b)* constraints in the ϕ_2 - $P/(|P|+|T|)$ plane for all values of δ. The dark blue region corresponds to 1σ C.L., the light blue region to 90% C.L., and the green region to 95% C.L.

parameters (including $\mathcal{C}_{\pi\pi}$ and $\mathcal{S}_{\pi\pi}$) in the fit.

The Belle and BaBar results can be averaged together to constrain ϕ_2. However, such a constraint requires knowledge or assumptions about $|P/T|$ or δ. A model based on $SU(3)$ symmetry (and including an $SU(3)$-breaking factor f_K/f_π for tree amplitudes) and the measured rates for $B^0 \to K^0\pi^+$ and $B^0 \to K^+\pi^-$ indicates $\phi_2 = (103 \pm 17)^\circ$ [18] (note: this uses the BaBar result for 113 fb^{-1} of data). A preferred method is to use isospin symmetry and the measured rates for $B^+ \to \pi^+\pi^0$, $B^0 \to \pi^0\pi^0$, and charge-conjugates; this method can determine ϕ_2 with little theoretical uncertainty [19]. However, the decay $B^0 \to \pi^0\pi^0$ has only recently been observed and the asymmetry between B^0 and $\overline{B}{}^0$ measured [20]. Future measurements with higher statistics should yield an interesting constraint on ϕ_2. The overall $(B^0 + \overline{B}{}^0) \to \pi^0\pi^0$ branching fraction can be used to obtain an upper bound [21] on the angular difference $\theta \equiv \phi_2 - \phi_{2\,\mathrm{eff}}$, where $S_{\pi\pi} = \sin 2\phi_{2\,\mathrm{eff}}$ (i.e., $\phi_{2\,\mathrm{eff}} \to \phi_2$ as $P \to 0$). Using $\mathcal{C}_{\pi\pi}$ and the most recent values of the above branching fractions [11] fluctuated by 1σ in the conservative direction, one obtains $\theta < 36^\circ$.

4. $B^0 \to \rho^+\pi^-$

For $B^0 \to \rho^+\pi^-$, the final state is not a CP eigenstate. There are thus four separate decays to consider: $B^0 \to \rho^\pm\pi^\mp$ and $\overline{B}{}^0 \to \rho^\pm\pi^\mp$. The decay rates can be parametrized as [22]

$$\frac{dN(B \to \rho^\pm\pi^\mp)}{d\Delta t} \propto (1 \pm A_{CP}^{\rho\pi}) \times e^{-\Delta t/\tau}\Big[1 - q\,(\mathcal{C}_{\rho\pi} \pm \Delta\mathcal{C}_{\rho\pi})\cos(\Delta m \Delta t) + q\,(\mathcal{S}_{\rho\pi} \pm \Delta\mathcal{S}_{\rho\pi})\sin(\Delta m \Delta t)\Big], \quad (5)$$

where $q = +1$ ($q = -1$) corresponds to B^0 ($\overline{B}{}^0$) tags. The parameters $\mathcal{C}_{\rho\pi}$ and $\mathcal{S}_{\rho\pi}$ are CP-violating, while the parameters $\Delta\mathcal{C}_{\rho\pi}$ and $\Delta\mathcal{S}_{\rho\pi}$ are CP-conserving. $\Delta\mathcal{C}_{\rho\pi}$ characterizes the difference in rates between "$W \to \rho$" processes $B^0 \to \rho^+\pi^-$ or $\overline{B}{}^0 \to \rho^-\pi^+$ and "spectator $\to \rho$" processes $B^0 \to \rho^-\pi^+$ or $\overline{B}{}^0 \to \rho^+\pi^-$ (see Fig. 1). $\Delta\mathcal{S}_{\rho\pi}$ depends, in addition, on differences in

phases between $W \to \rho$ and spectator $\to \rho$ amplitudes.

The parameter $A_{CP}^{\rho\pi}$ is equal to the time and flavor integrated asymmetry: $\Gamma(B^0 \to \rho^+\pi^-) + \Gamma(\overline{B}{}^0 \to \rho^+\pi^-) - \Gamma(\overline{B}{}^0 \to \rho^-\pi^+) - \Gamma(B^0 \to \rho^-\pi^+)$ divided by the sum of the four rates. We also define two separate CP asymmetries:

$$A_{+-} \equiv \frac{N(\overline{B}{}^0 \to \rho^-\pi^+) - N(B^0 \to \rho^+\pi^-)}{N(\overline{B}{}^0 \to \rho^-\pi^+) + N(B^0 \to \rho^+\pi^-)} = -\frac{A_{CP}^{\rho\pi} + C_{\rho\pi} + A_{CP}^{\rho\pi} \cdot \Delta C_{\rho\pi}}{1 + \Delta C_{\rho\pi} + A_{CP}^{\rho\pi} \cdot C_{\rho\pi}} \quad (6)$$

and

$$A_{-+} \equiv \frac{N(\overline{B}{}^0 \to \rho^+\pi^-) - N(B^0 \to \rho^-\pi^+)}{N(\overline{B}{}^0 \to \rho^+\pi^-) + N(B^0 \to \rho^-\pi^+)} = \frac{A_{CP}^{\rho\pi} - C_{\rho\pi} - A_{CP}^{\rho\pi} \cdot \Delta C_{\rho\pi}}{1 - \Delta C_{\rho\pi} - A_{CP}^{\rho\pi} \cdot C_{\rho\pi}} \ . \quad (7)$$

A_{+-} depends only on $W \to \rho$ processes and A_{-+} depends only on spectator $\to \rho$ processes.

Both BaBar and Belle have done unbinned ML fits to the Δt distributions of $B^0 \to \rho^\pm\pi^\pm$ decays to determine $A_{CP}^{\rho\pi}$, $\mathcal{C}_{\rho\pi}$, $\mathcal{S}_{\rho\pi}$, $\Delta\mathcal{C}_{\rho\pi}$, $\Delta\mathcal{S}_{\rho\pi}$, A_{+-}, and A_{-+}. The Belle analysis is with 140 fb^{-1} of data [23]; the BaBar analysis, originally with 81 fb^{-1} of data [24], has been updated with 113 fb^{-1} [25].

To remove charge-ambiguous decays and possible interference between $B^0 \to \rho^+\pi^-$ and $B^0 \to \rho^-\pi^+$ amplitudes, one must eliminate the overlap region of the $\pi^+\pi^-\pi^0$ Dalitz plot. Belle does this by requiring $0.57\ \mathrm{GeV}/c^2 < m_{\pi^\pm\pi^0} < 0.97\ \mathrm{GeV}/c^2$ and $m_{\pi^\mp\pi^0} > 1.22\ \mathrm{GeV}/c^2$. BaBar makes the looser selection $0.40\ \mathrm{GeV}/c^2 < m_{\pi^\pm\pi^0} < 1.30\ \mathrm{GeV}/c^2$ and requires that $m_{\pi^\mp\pi^0}$ not be in this range. In addition, BaBar requires that the bachelor track from $B \to \rho\pi$ has $p > 2.4\ \mathrm{GeV}/c$, where p is evaluated in the e^+e^- CM frame; only 14% of pions from (selected) $\rho^\pm$ decays satisfy this requirement. Finally, Belle requires $m_{\pi^+\pi^-} > 0.97\ \mathrm{GeV}/c^2$ to avoid the overlap region between $B^0 \to \rho^0\pi^0$ and $B^0 \to \rho^\pm\pi^\mp$.

Belle subsequently defines a signal region $m_{\rm bc} > 5.27\ \mathrm{GeV}/c^2$ and $-0.10\ \mathrm{GeV} < \Delta E < 0.08\ \mathrm{GeV}$. There are 1215 events in this region that pass all selection requirements. Fitting to the $m_{\rm bc}$-ΔE distributions yields 329 $B^0 \to \rho^+\pi^-$ candidates. The resulting Δt distributions for $q = \pm 1$ tagged events are shown in Fig. 4 along with projections of the unbinned ML fit in Δt. Also shown is the CP asymmetry, which is consistent with zero.

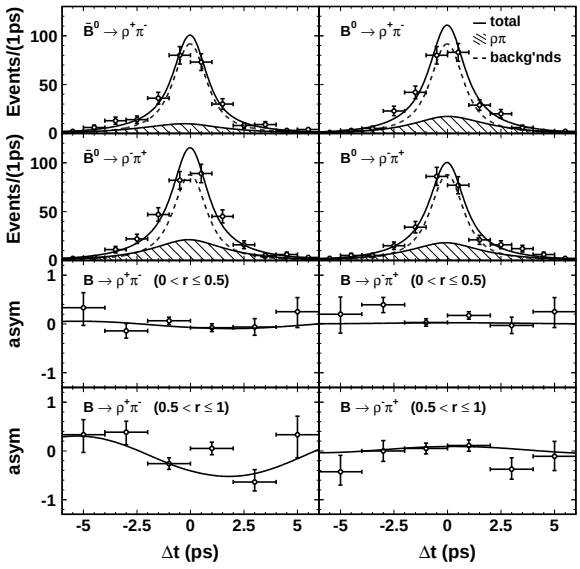

Figure 4. Belle results for $B^0 \to \rho^+\pi^-$ [23]: the Δt distributions of $q = 1$ tags (left), $q = -1$ tags (right), and the resulting CP asymmetry (bottom rows). The asymmetry is shown separately for high-quality tags ($r > 0.5$) and low quality tags ($r < 0.5$). The smooth curves are projections of the unbinned ML fit.

The BaBar results are similar to those from Belle; the corresponding Δt distributions and CP asymmetry are shown in Fig. 5. All Belle and BaBar results are listed in Table 1. There is very good agreement between the measurements except for $\Delta\mathcal{S}_{\rho\pi}$, where the disagreement is $\sim 2\sigma$. A recent BaBar analysis with 192 fb^{-1} of data [26] uses a different strategy than the quasi-two-body approach: it takes advantage of interference in the $\pi^+\pi^-\pi^0$ Dalitz plot as prescribed in Ref. [27]. These results are also listed in Table 1 for comparison; they are very similar to those from the quasi-two-body analyses.

These measured values can be used to constrain

Table 1
Results of fits to the Δt distributions for $B^0 \to \rho^+\pi^-$ candidates.

	Belle 2-body ($140\ \text{fb}^{-1}$)	**BaBar 2-body ($113\ \text{fb}^{-1}$)**	**BaBar Dalitz ($192\ \text{fb}^{-1}$)**
$A_{CP}^{\rho\pi}$	$-0.16 \pm 0.10 \pm 0.02$	$-0.114 \pm 0.062 \pm 0.027$	$-0.088 \pm 0.049 \pm 0.013$
$C_{\rho\pi}$	$0.25 \pm 0.17\,^{+0.02}_{-0.06}$	$0.35 \pm 0.13 \pm 0.05$	$0.34 \pm 0.11 \pm 0.05$
$S_{\rho\pi}$	$-0.28 \pm 0.23\,^{+0.10}_{-0.08}$	$-0.13 \pm 0.18 \pm 0.04$	$-0.10 \pm 0.14 \pm 0.04$
$\Delta C_{\rho\pi}$	$0.38 \pm 0.18\,^{+0.02}_{-0.04}$	$0.20 \pm 0.13 \pm 0.05$	$0.15 \pm 0.11 \pm 0.03$
$\Delta S_{\rho\pi}$	$-0.30 \pm 0.24 \pm 0.09$	$0.33 \pm 0.18 \pm 0.03$	$0.22 \pm 0.15 \pm 0.03$
A_{+-}	$-0.02 \pm 0.16\,^{+0.05}_{-0.02}$	$-0.18 \pm 0.13 \pm 0.05$	$-0.21 \pm 0.11 \pm 0.04$
A_{-+}	$-0.53 \pm 0.29\,^{+0.09}_{-0.04}$	$-0.52\,^{+0.17}_{-0.19} \pm 0.07$	$-0.47\,^{+0.14}_{-0.15} \pm 0.06$

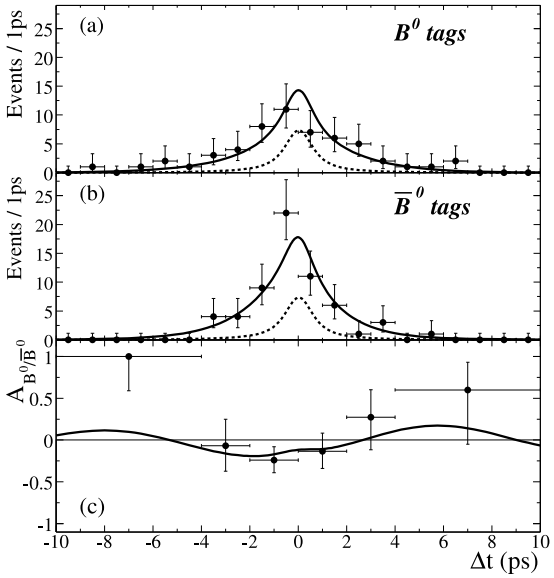

Figure 5. BaBar results for $B^0 \to \rho^+\pi^-$ [24]: the Δt distributions of $q = 1$ tags (top), $q = -1$ tags (middle), and the resulting CP asymmetry (bottom). The smooth curves are projections of the unbinned ML fit.

ϕ_2; however, since the penguin contribution is unknown, additional information is needed. A recent theoretical model [28] uses $SU(3)$ symmetry and the measured rates or limits for branching fractions of $B^0 \to K^{*\pm}\pi^{\mp}$, $B^0 \to \rho^{\mp}K^{\pm}$, $B^{\pm} \to K^{*0}\pi^{\pm}$, and $B^{\pm} \to \rho^{\pm}K^0$. $SU(3)$-breaking effects are considered at tree level and accounted for via a factor f_π/f_K. The strong phase difference between the two tree amplitudes ($W \to \rho$ and spectator$\to \rho$) is assumed to be small, as predicted by factorization. The resulting central values and errors for ϕ_2 are: $102 \pm 19°$ for Belle values of $\mathcal{C}_{\rho\pi}$, $\mathcal{S}_{\rho\pi}$, $\Delta\mathcal{C}_{\rho\pi}$, $\Delta\mathcal{S}_{\rho\pi}$; $93 \pm 17°$ for BaBar values ($113\ \text{fb}^{-1}$); and $95 \pm 16°$ for Belle and BaBar values combined.

The BaBar Dalitz plot analysis ($192\ \text{fb}^{-1}$) [26] allows one to directly fit for ϕ_2 with little theoretical uncertainty from the penguin contribution. The result is $\phi_2 = (113\,^{+27}_{-17}\,(\text{stat}) \pm 6\,(\text{syst}))°$, consistent with the $SU(3)$-based results above.

5. $B^0 \to \rho^+\rho^-$

The decay $B^0 \to \rho^+\rho^-$ has two vector particles in the final state. If the ρ mesons are longitudinally polarized, ℓ is even and $CP = +1$; but if they are transversely polarized, ℓ can be even or odd and the final state is not a CP eigenstate.

For longitudinal polarization, ϕ_2 can be determined from the Δt distribution as done for $B^0 \to \pi^+\pi^-$. However, $B^0 \to \rho^+\rho^-$ has an advantage: the penguin contribution is expected to be small relative to the tree contribution [29], which

reduces theoretical uncertainty on ϕ_2. Unfortunately $B^0 \to \rho^+\rho^-$ is more challenging experimentally: there are several backgrounds and also possible nonresonant contributions. The method depends upon the ρ's being longitudinally polarized; otherwise a more involved angular analysis is necessary to determine ϕ_2 [30]. Finally, the nonnegligible decay width of the ρ allows for $I = 1$ final states, which complicates extracting ϕ_2 via an isospin analysis [31].

The decay $B^0 \to \rho^+\rho^-$ has been observed by BaBar and the CP-violating parameters $\mathcal{C}_{\rho\rho}$ and $\mathcal{S}_{\rho\rho}$ measured with 81 fb^{-1} of data [7,8] and updated with 113 fb^{-1} of data [25]. A similar analysis is underway at Belle with 250 fb^{-1} of data. The final state consists of four pions, two charged and two neutral. In the case of multiple $B^0 \to \rho^+\rho^-$ candidates arising from multiple π^0 candidates, the candidate that minimizes the sum $\sum_i (m^{(i)}_{\gamma\gamma} - m_{\pi^0})$ is chosen, where i runs over the $\rho^\pm$ candidates. From MC simulation, it is found that one or more pions from $B^0 \to \rho^+\rho^-$ are swapped with pions from the tag side 39% (16%) of the time for longitudinal (transverse) polarization.

BaBar selects events with relatively loose cuts and does an unbinned ML fit to the Δt distribution, including pdf's to account for backgrounds. Nonresonant contributions and interference with decays yielding the same final state, e.g., $B^0 \to a_1\pi^0$, are estimated to be small and neglected. For 81 fb^{-1} of data, 24 288 events are fit and a signal yield of 224 ± 29 is obtained. The fit includes a pdf for the angles θ_1 and θ_2, where θ_i is the angle between the π^0 from $\rho_i^\pm \to \pi^\pm\pi^0$ and the B^0 in the $\rho_i^\pm$ rest frame ($i = 1, 2$). This pdf has the form [32]

$$\frac{d^2\Gamma}{\Gamma\, d\cos\theta_1\, d\cos\theta_2} = \frac{9}{4}\Big\{ f_L \cos^2\theta_1 \cos^2\theta_2 + \left(\frac{1-f_L}{4}\right)\sin^2\theta_1 \sin^2\theta_2 \Big\} \quad (8)$$

and determines f_L, the fraction of longitudinally polarized decays. The fit results are $\mathcal{C}_{\rho\rho} = -0.23 \pm 0.24 \pm 0.14$ and $\mathcal{S}_{\rho\rho} = -0.19 \pm 0.33 \pm 0.11$ (113 fb^{-1}), and $f_L = 0.99 \pm 0.03\,^{+0.04}_{-0.03}$ (81 fb^{-1}). The first error listed is statistical and the second systematic.

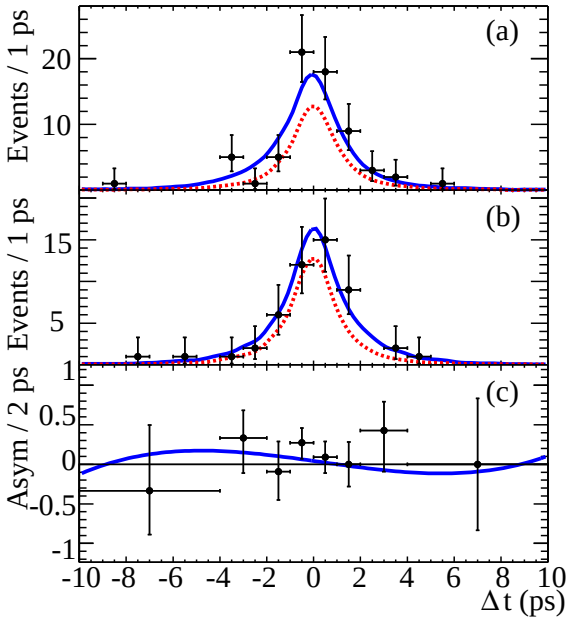

Figure 6. BaBar results for $B^0 \to \rho^+\rho^-$ [7]: the Δt distributions of $q = 1$ tags (top), $q = -1$ tags (middle), and the resulting CP asymmetry (bottom). The smooth curves are projections of the unbinned ML fit.

It is fortunate that f_L is close to unity; in this case the final state has $CP = +1$ and an angular analysis to determine ϕ_2 is unnecessary. Fig. 6 shows the Δt distributions for $q = \pm 1$ tagged events along with the resulting CP asymmetry. No CP violation is observed. Inputting the measured values for $\mathcal{C}_{\rho\rho}$ and $\mathcal{S}_{\rho\rho}$ into an isospin analysis that includes the branching fractions for $B^0 \to \rho^+\rho^-$ [7] and $B^+ \to \rho^+\rho^0$ [33], and the upper limit for $B(B^0 \to \rho^0\rho^0)$ [34], one obtains $\phi_2 = (96 \pm 10\,(\text{stat}) \pm 4\,(\text{syst}) \pm 11_{\text{theory}})^\circ$ [35]. The last error is due to the penguin contribution; it is significantly smaller than that for $B \to \pi\pi$ ($\pm 36^\circ$), as expected.

6. SUMMARY

Time-dependent CP asymmetries in $B^0 \to \pi^+\pi^-$, $B^0 \to \rho^+\pi^-$, and $B^0 \to \rho^+\rho^-$ decays are

measured and used to constrain the CKM angle ϕ_2. The $B^0 \to \pi^+\pi^-$ mode is experimentally clean but has the largest penguin contribution, which contributes theoretical uncertainty to ϕ_2. A model-independent constraint is $90^\circ < \phi_2 < 146^\circ$ for $|P/T| < 0.45$ (95% C.L.). An $SU(3)$-based model [18] indicates $\phi_2 = (103 \pm 17)^\circ$ (and also that $|P/T|$ is large). Belle observes large CP violation in this mode while BaBar does not.

The $B^0 \to \rho^\pm\pi^\mp$ mode is more complicated as there are more backgrounds than for $B^0 \to \pi^+\pi^-$ and the final state is not a CP eigenstate. A model based upon $SU(3)$ symmetry and using the measured branching fractions for $B \to K^*\pi^\pm$ and $B \to \rho^\pm K$ obtains $\phi_2 = 95 \pm 16^\circ$ (Belle + BaBar quasi-two-body results combined).

The $B^0 \to \rho^+\rho^-$ mode has the smallest penguin contribution but suffers from additional backgrounds, possible nonresonant contributions, and a possible $I = 1$ component in the final state. Neglecting the latter two effects, BaBar measures $\mathcal{C}_{\rho\rho}$ and $\mathcal{S}_{\rho\rho}$ for longitudinal polarization, which dominates the decay. Combining the measured values with the branching fractions or limits for $B^0 \to \rho^+\rho^-$ [7], $B^+ \to \rho^+\rho^0$ [33], and $B^0 \to \rho^0\rho^0$ [34] gives $\phi_2 = (96 \pm 10\,(\text{stat}) \pm 4\,(\text{syst}) \pm 11_{\text{theory}})^\circ$ [35]. This value is similar to those obtained from measurements of $B^0 \to \pi^+\pi^-$ and $B^0 \to \rho^\pm\pi^\mp$ decays.

REFERENCES

1. http://belle.kek.jp/
2. http://www.slac.stanford.edu/BFROOT/
3. B. Aubert *et al.*, Nucl. Instr. Meth. A 479 (2002) 1.
4. A. Abashian *et al.*, Nucl. Instr. Meth. A 479 (2002) 117.
5. G. C. Fox and S. Wolfram, Phys. Rev. Lett. 41 (1978) 1581.
6. B. Casey *et al.*, Phys. Rev. D 66 (2002) 092002.
7. B. Aubert *et al.*, Phys. Rev. D 69 (2004) 031102.
8. B. Aubert *et al.*, hep-ex/0404029 (2004).
9. M. Gronau, Phys. Rev. Lett. 63 (1989) 1451.
10. M. Gronau and J. L. Rosner, Phys. Rev. D 65 (2002) 093012.
11. http://www.slac.stanford.edu/xorg/hfag/
12. K. Abe *et al.*, Phys. Rev. Lett. 93 (2004) 021601.
13. K. Abe *et al.*, Phys. Rev. D 68 (2003) 012001.
14. M. Beneke *et al.*, Nucl. Phys. B 606 (2001) 245; M. Beneke and M. Neubert, Nucl. Phys. B 675 (2003) 333.
15. Y. Y. Keum and A. A. Sanda, Phys. Rev. D 67 (2003) 054009.
16. B. Aubert *et al.*, Phys. Rev. Lett. 89 (2002) 281802.
17. B. Aubert *et al.*, hep-ex/0408089 (2004).
18. M. Gronau and J. L. Rosner, Phys. Lett. B 595 (2004) 339.
19. M. Gronau and D. London, Phys. Rev. Lett. 65 (1990) 3381.
20. K. Abe *et al.*, hep-ex/0408101 (2004).
21. M. Gronau *et al.*, Phys. Lett. B 514 (2001) 315; J. Charles, Phys. Rev. D 59 (1999) 054007; Y. Grossman and H. R. Quinn, Phys. Rev. D 58 (1998) 017504.
22. M. Gronau, Phys. Lett. B 233 (1989) 479.
23. C. C. Wang *et al.*, hep-ex/0408003 (2004).
24. B. Aubert *et al.*, Phys. Rev. Lett. 91 (2003) 201802.
25. L. Roos (for BaBar), hep-ex/0407051 (2004).
26. B. Aubert *et al.*, hep-ex/0408099 (2004).
27. H. R. Quinn and A. E. Snyder, Phys. Rev. D 48 (1993) 2139.
28. M. Gronau and J. Zupan, hep-ph/0407002 (2004).
29. R. Aleksan *et al.*, Phys. Lett. B 356 (1995) 95.
30. I. Dunietz *et al.*, Phys. Rev. D 43 (1991) 2193.
31. A. F. Falk *et al.*, Phys. Rev. D 69 (2004) 011502.
32. K. Abe, M. Satpathy, and H. Yamamoto, hep-ex/0103002 (2001).
33. J. Zhang *et al.*, Phys. Rev. Lett. 91 (2003) 221801; B. Aubert *et al.*, Phys. Rev. Lett. 91 (2003) 171802.
34. B. Aubert *et al.*, hep-ex/0408061 (2004).
35. M. A. Giorgi, "Recent Results on CP Violation in B Decays," presented at *XXXII Int. Conf. on High Energy Physics,* Beijing, China, 16-22 August 2004.